Macromolecular Research, Vol. 16, No. 7, pp 644-650 (2008)

Mechanical Behavior of Shape Memory Fibers Spun from Nanoclay-Tethered Polyurethanes

Seok Jin Hong and Woong-Ryeol Yu*

Department of Materials Science and Engineering, Seoul National University, Seoul 151-742, Korea

Ji Ho Youk

Department of Advanced Fiber Engineering, Division of Nano-System, Inha University, Incheon 402-751, Korea

Received March 20, 2008; Revised June 13, 2008; Accepted June 19, 2008

Abstract: This study examined the effect of nanoclays on the shape memory behavior of polyurethane (PU) in fibrous form. A cation was introduced into the PU molecules to disperse the organo-nanoclay (MMT) into poly(ε-caprolactone) (PCL)-based PU (PCL-PU). The MMT/PCL-PU nanocomposites were then spun into fibers through melt-processing. The shape memory performance of the spun fibers was examined using a variety of thermo-mechanical tests including a new method to determine the transition temperature of shape memory polymers. The MMTs showed an improved the fixity strain rate of the MMT/PCL-PU fibers but a slight decrease in their recovery strain rate. This was explained by the limited movement of PU molecules due to the presence of nanoclays. The shape memory performance of the MMT/PCL-PU fibers was not enhanced significantly by the nanoclays. However, their recovery power was improved significantly up to a strain of approximately 50%.

Keywords: shape memory polymers, polyurethane, fibers, nanoclay.

Introduction

Polyurethanes (PUs) are versatile polymers on account of their excellent properties such as high abrasion resistance, good tear strength, excellent shock absorption, and flexible and large elastic behavior. However, they suffer from low thermal stability and barrier properties.[1] Such unfavorable properties can be tailored and improved by introducing filler particles, such as nanoclays, which can influence the mechanical properties including the shape memory behavior.[2]

Due to their phase separated hard and soft segments, polyurethanes feature a shape memory behavior, i.e., an ability to return to their original shape from a strained and temporarily fixed one when heated above the transition temperature. The shape memory behavior of polyurethanes results from the entropic elastic behavior of the soft segment in the rubbery state above the transition temperature.[3] The transition temperature, above which the soft segment is in a rubbery state, is determined by the melting temperature (T_m) or the glass transition temperature (T_g) of the soft segment depending on whether the polymer molecules in the soft segment can form crystallites or not.[4,5]

*Corresponding Author. E-mail: woongryu@snu.ac.kr

Shape memory polymers (SMPs) have many advantages, such as easy processing to complex parts, low manufacturing cost, low density, and high shape recovery strain.[6-8] SMPs show high levels of recovery strains larger than 100%, whereas shape memory metals or ceramics can recover several percentage points of deformation at most. While the stress developed when the materials are not subject to deformation upon heating, i.e., recovery stress, is usually 1-3 MPa for shape memory polymers, Ti-Ni shape memory alloys show a range of 200-400 MPa stress. High recovery stress and immediate recovery in shape memory alloys make them unfavorable for deployable structures, e.g., biomedical devices, due to the imminent damage to the auxiliary equipment. Therefore, the relatively slow shape recovery of shape memory polymers may provide better alternatives for the deployable structures. However a small recovery stress is the main obstacle to their wide application in deployable structures. Recently, considerable effort has been made to obtain higher recovery stress by reinforcing SMPs with stiff fibers or particulate fillers, such as clay and carbon nanotubes.[9,10]

The aim of this study was to improve the recovery stress of SMPs by introducing nanoclay and to investigate their mechanical properties after they are processed, particularly in fibrous form. For this purpose, the nanoclay dispersed

SMPs were prepared and spun into fibers. The thermomechanical and other tests, such as DSC, XRD, and static tensile tests, were carried out to determine the effect of the nanofillers on the mechanical behavior of shape memory fibers.

Experimental

Materials. Poly(ε-caprolactone) (PCL, $M_n \approx 2{,}000$), 4,4′-diphenylmethylene diisocyanate (MDI), 1,4-butanediol (BD), *N*-methyldiethanolamine (MDEA), dibutyltin dilaurate, iodomethane, *N,N*-dimethyl formamide (DMF), tetrahydrofuran (THF) were used as received from Aldrich. Cloisite-30B, an organically modified MMT (O-MMT), was provided by Southern Clay. The PCL and Cloisite-30B were dried overnight at 90 °C to remove the moisture prior to use.

A two-step procedure was used to synthesize PCL-based PU (PCL-PU). In the first step, the isocyanate terminated prepolymers were synthesized by reacting PCL with an excess of MDI at 50 °C for 1.5 h under a nitrogen atmosphere. In the second step, dibutyltin dilaurate was added to the prepolymers as a catalyst. The chain extension of the prepolymers was reacted by adding BD or BD and MDEA dissolved in DMF drop wise. The reaction temperature was slowly increased to 80 °C and kept at this temperature for 2 h with constant stirring. The subsequent molar ratios of MDI/BD/PCL and MDI/BD/PCL/MDEA were 4.0/3.0/1.0 and 4.0/2.6/1.0/0.4 for the PCL-PU and cationic PCL-PU, respectively. For the cationic PCL-PU, the additional quaternization of the PCL-PU main chains was carried out by introducing 1.0 equiv. of iodomethane for 1.0 equiv. of MDEA.

Preparation of MMT/PCL-PU Nanocomposites and Their Melt-Spinning. MMT/PCL-PU nanocomposites were prepared using a solution blending method in which the cationic PCL-PU was dissolved in DMF at a concentration of 0.1 g/mL. A predetermined amount of Cloisite-30B was then dispersed in 50 mL of DMF and ultra-sonicated for 1.5 h. The dispersion was added to the PCL-PU solution and stirred at 80 °C for further 2 h. The resulting MMT/PCL-PU solution was poured into a glass dish and dried slowly at 45 °C. Due to the introduced cation, the MMT was dispersed in PCL-PU up to its 20 wt%. This nanocomposite was used as a master batch, i.e., it was compounded with PCL-PU by a twin extruder to prepare the melt-spinning chips with nanoclay contents of 0.25, 0.5, 0.75, and 1.00 wt%. The MMT/PCL-PU fibers were then produced using a spinning system (RCP-0500 Microtruder, Randcastle Extrusion Systems, Inc) (see Table I for details of the processing conditions). Note that the temperature conditions of PCL-PU without MMTs were set up slightly different from those of MMT/PCL-PU nanocomposites because MMTs in PCL-PU influence the melt flow of MMT/PCL-PU nanocomposites.

Characterizations. Wide angle X-ray diffraction (WAXD) analysis was carried out using a Rigaku DMAX-2500 diffractometer to measure the *d*-spacing of MMTs in PCL-PU. Each sample was scanned from $2\theta = 1$ to 10° at a scan rate of 0.01°/min. The wavelength of the X-ray beam was 0.154 nm (CuK_α radiation). For MMT/PCL-PU fibers, wide angle X-ray diffractograms were recorded on a GADDS diffractometer from Bruker. The scanning range was 0° to 40° at a scan rate of 20°/min. The wavelength of the beam was 0.154 nm (CuK_α line).

The thermal properties of the PCL-PU and MMT/PCL-PU were measured using a thermal analyzer (DSC823e, METTLER TOLEDO Ltd.) with a DSC module purged with nitrogen gas, and quenched with liquid nitrogen. The specimens were scanned from -80 to 220 °C in sealed aluminum pans at a heating rate of 10 °C/min.

Thermo-Mechanical Test. The thermal mechanical tests of the MMT/PCL-PU nanocomposite fibers were carried out by modifying the tensile testing mode of DMTA, as shown in Figure 1 (see also Table II for details of the test condition). The fibrous specimens with a gauge length of 5 mm were stretched at a strain rate of 100% per min (crosshead speed 5 mm/min). At temperatures (T_h) higher than the transition temperature (T_{tr}), the MMT/PCL-PU fibers were deformed mechanically into a temporary shape (stage ① in Figure 1). The temporary shape was fixed by lowering the temperature (T_l, stage ② in Figure 1) and releasing the stress (stage ③ in Figure 1). At this time, the polymer molecules in the fibers tended to return to the permanent shape without deformation. However, since the rigidity in the molecules was increased by lowering the temperature, they

Table I. Melt Spinning Conditions of MMT/PCL-PU Nanocomposites

MMT wt%	Extruder Temperature (°C)				Screw Speed (rpm)	Winder Speed (rpm)	Draw Ratio*[2]
	Zone 1	Zone 2	Zone 3	Die			
0.0	185	190	195	195	60 (2.5*[1])	300 (75*[1])	30
0.25	172	177	182	182	60 (2.96)	300 (75)	25.34
0.50	172	177	182	182	60 (3.08)	300 (75)	24.35
0.75	172	177	182	182	60 (2.77)	300 (75)	27.08

[1]Values in the parenthesis are the linear velocity of the fibers at the die exit and the winder, respectively, and their ratio represent the draw ratio[2].

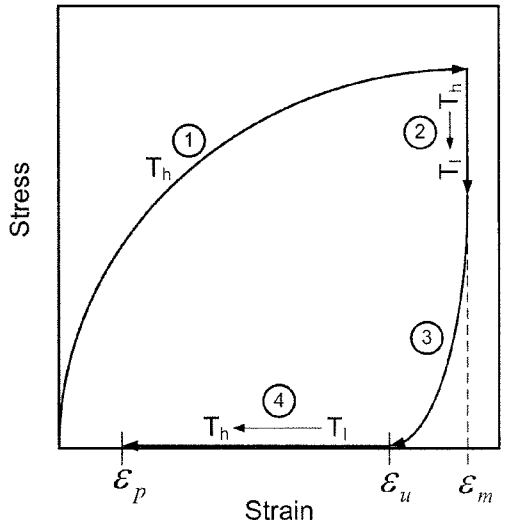

Figure 1. Thermo-mechanical test cycle of MMT/PCL-PU nanocomposite fibers.

Table II. Test Conditions for Shape Memory Performance Using DMTA

Step	Test (Mode)	Temperature (T_h=46 °C, T_l = 6 °C)
1	Tensile deformation	Keeping T_h
2	Stress relaxation (keeping the deformation fixed)	Cooling from T_h to T_l
3	Unloading (releasing stress to zero)	Keeping T_l
4	Zero load recovery (keeping stress to zero)	Heating from T_l to T_h

could not take up all the deformation, thereby leaving the temporary shape fixed. Here, the strain fixity rate can be defined as the difference in shape after stages ①and ③, and it can be a criterion for assessing the shape memory performance because a large strain fixity rate indicates better micro-phase separation in the SMPs. Upon heating, the rigidity of the polymer chains in the soft-segment decreased, and the frozen stress became activated such that SMP recovered all the deformation and returns to its permanent shape (stage ④ in Figure 1). Here, the strain recovery rate also can be a criterion for assessing the shape memory performance as follows:

$$\text{Strain fixity rate (\%)} = \frac{\varepsilon_u}{\varepsilon_m} \times 100 \quad (1)$$

$$\text{Strain recovery rate (\%)} = \frac{\varepsilon_m - \varepsilon_p}{\varepsilon_m} \times 100 \quad (2)$$

Results and Discussion

WAXD and Thermal Analysis. The exfoliation of nanoclays in PCL-PU through the cation was examined using the

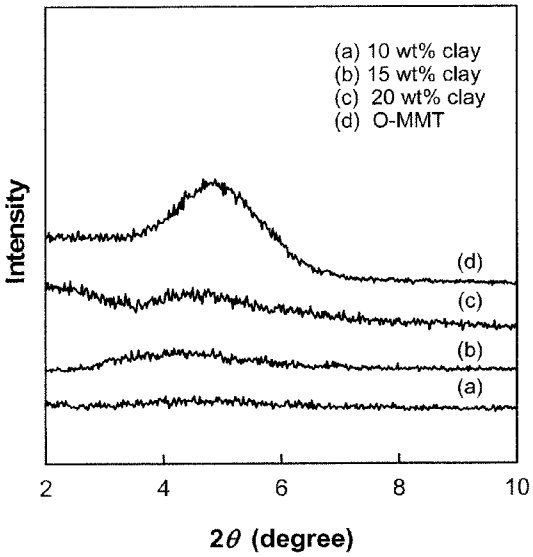

Figure 2. WAXD patterns of Cloisite-30B and the MMT/PCL-PU nanocomposites according to nanoclays contents.

WAXD patterns of both the nanoclays (Cloisite-30B) and their nanocomposites (see Figure 2). The 2θ peak of the nanoclay disappeared in MMT/PCL-PU nanocomposites. This showed that MMT is well dispersed and exfoliated up to its 20 wt%.[11] The fibers spun from the MMT/PCL-PU nanocomposites, which were prepared by compounding a MMT/PCL-PUs with MMT contents of 20 wt%, were also examined to check the exfoliation of nanoclays inside the fibers (see Figure 3). As in the nanocomposites, the nanoclays in the fibers can be considered well dispersed in that there was no diffraction peak. Note that the diffraction peak at $2\theta = 20°$ and its area decrease gradually with increasing MMT level (see from Figure 3), implying that the degree of crystallization decreases due to MMT intervention with the PU molecules.

The thermal characterizations of PCL-PU and MMT/PCL-PU nanocomposites were carried out using DSC (see Table III for thermogram and for its numeric values). Two noticeable features can be identified. First, the melting (T_m) and crystallization (T_c) temperatures were increased as the MMT contents in the PCL-PUs increased. This suggests that the MMTs act as a nucleating agent and contribute to increasing the crystallization temperature. However, they simultaneously reduce the crystallinityof the polymer by providing obstacles to crystal growth, which can be confirmed by the enthalpy values. Note that in contrast to the slight change in PCL-PUs with less than 0.75% MMT by weight, PCL-PU with a MMT content of 1.0 wt% shows a sharp decrease in the enthalpy of melting and crystallization, inducing that the crystallinity of PUs was further reduced by the increased nuclei and limited spaces. In addition, MMTs significantly influence the melt flow of MMT/PCL-PU nanocomposites in the spinning process, making

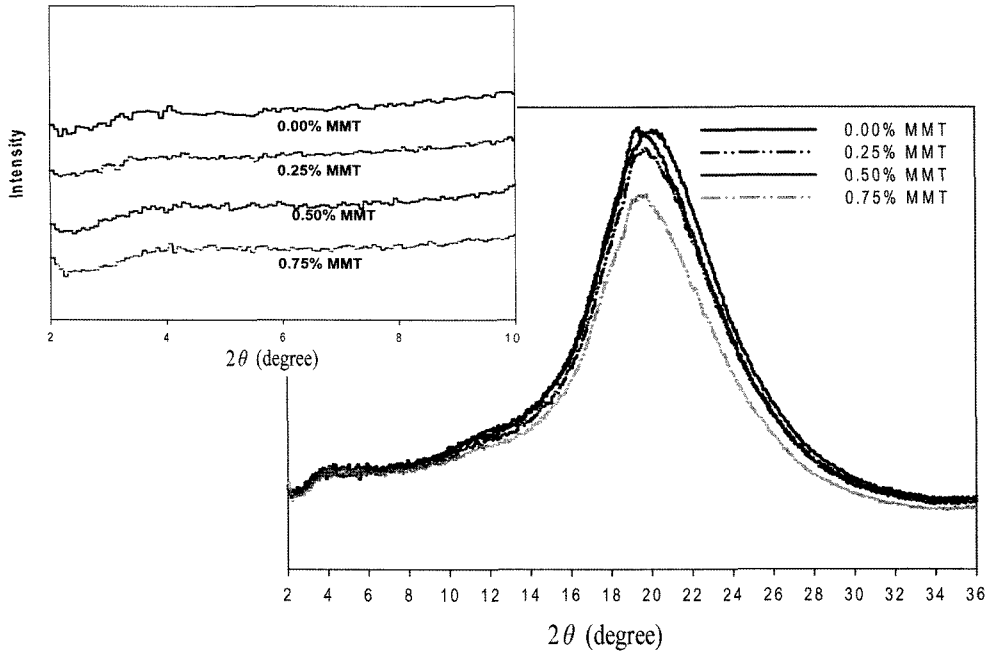

Figure 3. XRD patterns of the nanoclay-containing fibers made from MMT/PCL-PU nanocomposites.

the melt spinning of PCL-PU with a MMT content of 1 wt% impossible.

Second, although the melting temperature of PCL used for forming the soft segments in PCL-PU is approximately the room temperature, its melting peak was not observed in both PCL-PU and its nanocomposite (see Figure 4). This might be due to the low molecular weight of the PCL used and the relatively high hard-segment fraction because a low molecular weight of PCL may not crystallize due to hindrance by the hard segment when the hard segment fraction is relatively high.[12] In general, the crystallinity of the soft segment in polyurethanes increases with increasing length and content, due primarily to increased soft and hard segment phase separation. For polyurethanes with the same length of soft segment, the hard segment contents may determine the crystallinity of the soft segments because they obstruct the movement of the soft segment for crystallization.[5,13]

Transition Temperature of MMT/PCL-PU. In general, the transition temperature of SMPs can be determined by DSC and DMTA analysis. The melting temperature of the soft segment was not observed in the current SMPs. Therefore, the transition temperature of the PCL-PUs was measured using a new method based on their thermo-mechanical behavior. This method was developed by focusing on the fourth step of the thermo-mechanical test (see Figure 1), which is to measure the strain recovery rate by maintaining zero stress. For this zero stress, the cross head of the tensile testers should follow the sample contraction to release the stress caused by the increasing temperature. If the movement of the cross head does not match the sample contrac-

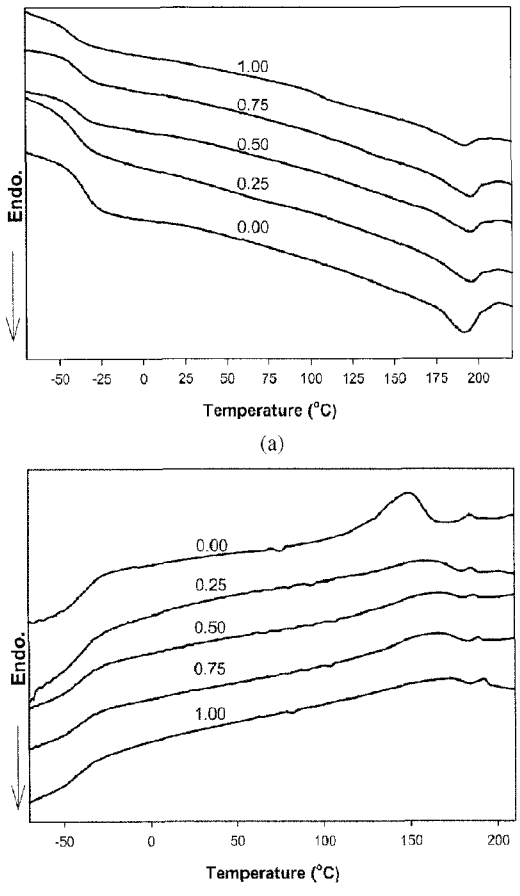

Figure 4. DSC thermogram of MMT/PCL-PU according to MMT contents.

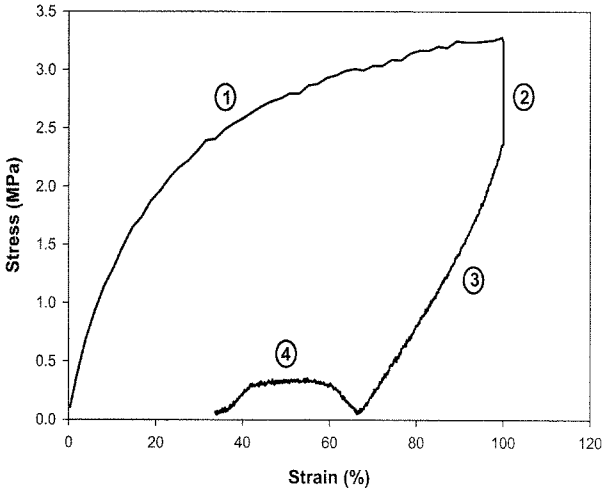

Figure 5. Stress developed at the fourth step of the thermo-mechanical test when the cross head speed does not match the material recovery (or contraction).

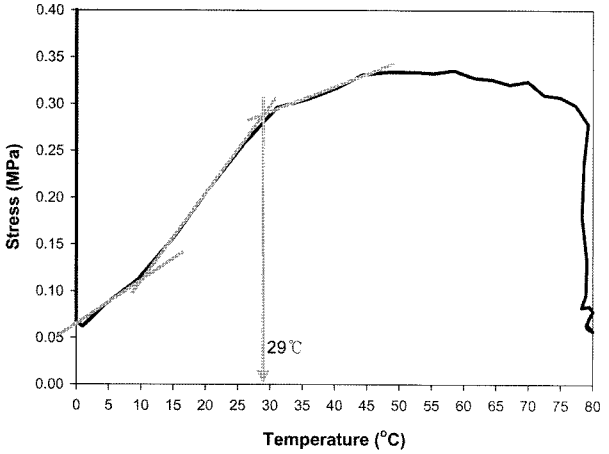

Figure 6. Stress vs. temperature curve at the fourth step of the modified thermo-mechanical test.

tion, a stress will develop due to a mismatch between the recovery strain and the crosshead movement. Figure 5 shows this thermo-mechanical behavior of SMPs when the cross head motion does not follow the material contraction

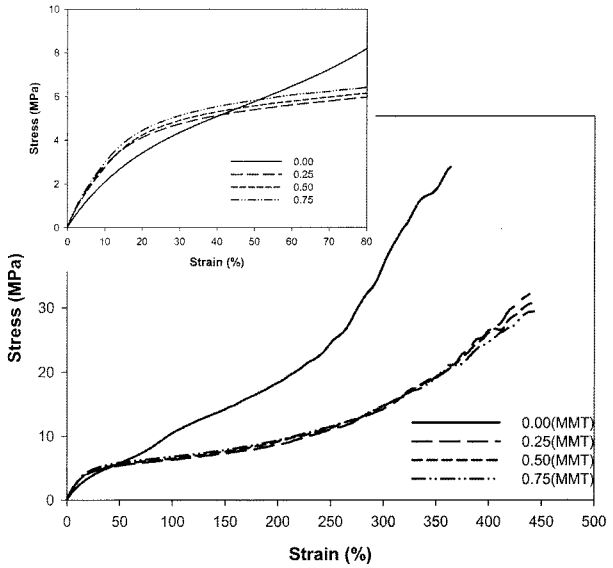

Figure 7. Tensile behavior of MMT/PCL-PU nanocomposite fibers at room temperature.

perfectly. As shown in Figure 6, the stress in the material increases slowly at the early part of heating and then increases sharply with the increasing temperature until a critical temperature. Then, the stress increased slowly. As a result, the critical temperature at which the rate of stress changes is severe can be regarded as the transition temperature of the SMPs. Based on this consideration, a temperature of 29 °C was determined to be the transition temperature of both PCL-PU and its nanocomposites.

Tensile and Thermo-Mechanical Behavior. The tensile behavior of the MMT/PCL-PU fibers was characterized by DMTA (Q-800, TA instruments). The fiber specimens (about 0.3 mm diameter) were strained up to 450% at a strain rate of 100% per min. Here the gauge length was set to 5 mm. As many research related with nanocomposite and its fibers shows the increases of the stiffness,[14-16] Figure 7 shows that the MMTs inside the PCL-PU improved the stiffness of the nanocomposite fibers up to 50% strain, beyond which, they decreased the stiffness. This decrease may be explained by MMTs that disturb the molecular orientation of PU mole-

Table III. Thermal Properties of MMT/PCL-PU Nanocomposites

Sample (MMT wt%)	Soft Segment	Hard Segment			
	T_g (°C)	T_m (°C)	T_c (°C)	ΔH_m^a (J/g)	ΔH_m^b (J/g)
	2nd	2nd	1st	2nd	1st
0.00	-36.83	191.38	149.62	5.29	5.24
0.25	-39.65	195.88	158.09	3.50	4.51
0.50	-38.70	194.94	168.08	4.02	3.86
0.75	-38.70	195.42	167.09	4.01	4.80
1.00	-42.15	192.4	172.08	2.84	1.84

1st, the first scan; 2nd, the second DSC scan. [a]Enthalpy of melting. [b]Enthalpy of crystallization.

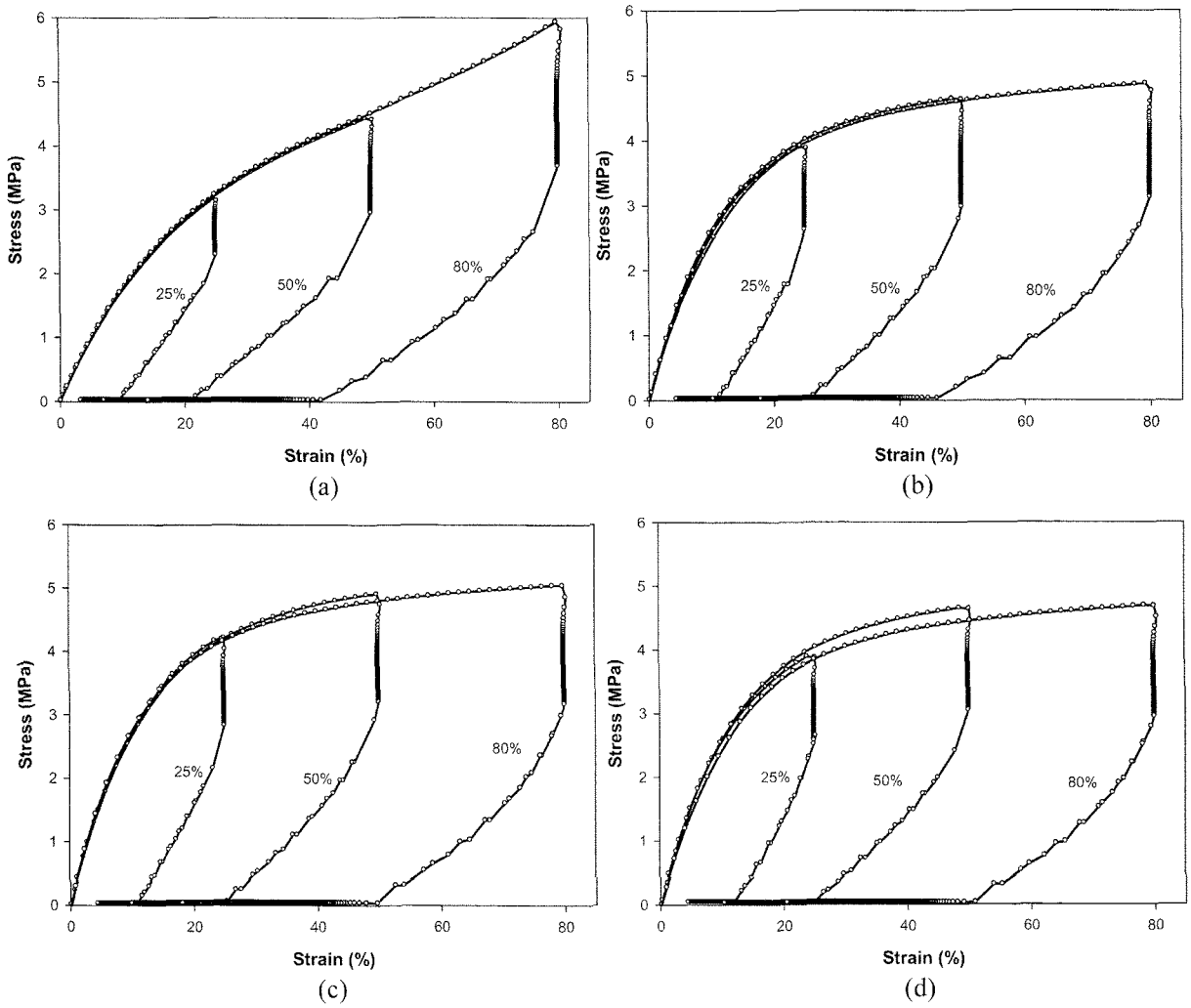

Figure 8. Thermo-mechanical behavior of SMP fibers according to the applied maximum strain. (a) MMT 0%, (b) MMT 0.25%, (c) MMT 0.50%, and (d) MMT 0.75%.

cules toward the tensile axis, which increases the stiffness in large deformation regime.

The thermo-mechanical test of the MMT/PCL-PU fibers was also carried out using DMTA based on the transition temperature, which was determined using the proposed method. At setting T_h (46 °C) and T_l (6 °C), the maximum strain at the first step in Figure 1 was varied to 25%, 50%, and 80%. For each applied strain, the thermo-mechanical cycle was imposed on the MMT/PCL-PU fibers according to the test conditions shown in Table II (see Figure 8). The shape memory performance of the MMT/PCL-PU fibers was evaluated by calculating the shape recovery and fixity strain rate from eqs. (1) and (2). Table IV shows that the shape memory performance of PCL-PU fibers was not as good as expected. On the other hand, the MMT improves the fixity strain rate, while it diminishes the recovery properties slightly. The effect of the nanoclays on the fixity and recovery strain ratio can be explained by the limited movement of PU molecules by the nanoclay. High temperature (T_h) weakens the interactions between the PU molecules as well as their interactions with the nanoclays, causing low

Table IV. Recovery and Fixity Strain Rate of MMT/PCL-PU Nanocomposite Fibers

Maximum Strain (%)		25%	50%	80%
Fixity R_f (%)	0.00 wt%	26.00	28.74	34.63
	0.25 wt%	30.15	35.09	40.76
	0.50 wt%	29.75	35.55	42.73
	0.75 wt%	31.40	36.35	43.30
Recovery R_r (%)	0.00 wt%	85.63	84.78	82.59
	0.25 wt%	81.97	79.51	76.96
	0.50 wt%	81.61	79.26	76.04
	0.75 wt%	81.45	78.56	75.79

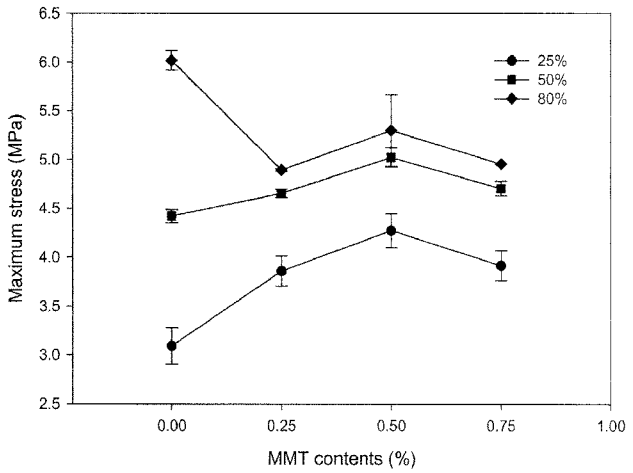

Figure 9. Maximum stress of MMT/PCL-PUC fibers in the thermo-mechanical test.

stiffness. As the strained fibers cools from T_h to T_l, the PCL units in the PCL-PU molecules in them become rigid because MMT obstruct the recovery motion of the soft-segments. As a result, the fixity strain rate of the MMT/PCL-PU fibers increases compared with that of the PCL-PU. When the fibers are in recovery motion at the fourth step of the thermo-mechanical cycle, MMT may interfere with the movement of soft segments, resulting in a poor recovery strain rate.

The maximum stress that develops as a result of the imposed strain in the first step of the thermo-mechanical cycle is also an important factor for determining the shape memory performance of the MMT/PCL-PU fibers because it is a proportional property to the recovery power. In Figure 9, the maximum stresses was plotted to examine the effects of the nanoclay on the recovery power. Along with MMT contents, the maximum stress clearly increases up to a certain fraction (e.g., 0.5), but it was lowered in the case of 0.75 wt% MMT, which might be due to relatively poor dispersion of MMTs in fibers compared to other two cases.

Conclusions

The shape memory fibers were manufactured by spinning PU containing nanoclays. The usage of the cationic PCL-PU molecules improved the dispersion of nanoclays in both PCL-PU and spun fibers. The effect of the nanoclays on the structure of the MMT/PCL-PU fibers and their subsequent mechanical properties were investigated by DSC, WAXD, and thermo-mechanical tests. MMT acts as a nucleation agent for crystallization, which increases the melting temperature, but obstructs the crystal growth. Regarding the thermo-mechanical behavior of shape memory polymers, a new method was proposed to determine the transition temperature when it cannot be clearly recognized in the DSC thermograms. Based on the transition temperature determined using this new method, the spun fibers from the MMT/PCL-PU nanocomposites were characterized by focusing on their shape memory performance. The fixity strain rate and the recovery power were enhanced by the nanoclays by limiting the movement of PU molecules.

Acknowledgement. This work was supported by the Korea Research Foundation Grant funded by the Korean Government (MOEHRD) (KRF-2006- 331-D00706).

References

(1) W. J. Choi, S. H. Kim, Y. Jin Kim, and S. C. Kim, *Polymer*, **45**, 6045 (2004).
(2) P. C. LeBaron, Z. Wang, and T. J. Pinnavaia, *Appl. Clay Sci.*, **15**, 11 (1999).
(3) A. Lendlein and S. Kelch, *Angew. Chem. Int. Edit.*, **41**, 2034 (2002).
(4) X. D. Guoqin Liu, Y. Cao, Z. Zheng, and Y. Peng, *Macromol. Rapid Comm.*, **26**, 649 (2005).
(5) B. K. Kim, S. Y. Lee, and M. Xu, *Polymer*, **37**, 5781 (1996).
(6) J. W. Cho and S. H. Lee, *Eur. Polym. J.*, **40**, 1343 (2004).
(7) C. Liu, H. Qin, and P. T. Mather, *J. Mater. Chem.*, **17**, 1543 (2007).
(8) S. Rezanejad and M. Kokabi, *Eur. Polym. J.*, **43**, 2856 (2007).
(9) F. Cao and S. C. Jana, *Polymer*, **48**, 3790 (2007).
(10) A. Lendlein and S. Kelch, *Clin. Hemorheol. Micro.*, **32**, 105 (2005).
(11) S. Sinha Ray and M. Okamoto, *Prog. Polym. Sci.*, **28**, 1539 (2003).
(12) P. Ping, W. Wang, X. Chen, and X. Jing, *Biomacromolecules*, **6**, 587 (2005).
(13) J. W. Cho, Y. C. Jung, Y.-C. Chung, and B. C. Chun, *J. Appl. Polym. Sci.*, **93**, 2410 (2004).
(14) J. C. Kim and J. H. Chang, *Macromol. Res.*, **15**, 449 (2007).
(15) S. Khvan, J. Kim, and S. S. Lee, *Macromol. Res.*, **15**, 51 (2007).
(16) Y. H. Kim, S. J. Choi, and J. M. Kim, *Macromol. Res.*, **15**, 676 (2007).